Part I

Defects and Modelling

DEFECT EVOLUTION IN ION IMPLANTED Si: FROM POINT TO EXTENDED DEFECTS

Sebania Libertino[a], Janet L. Benton[b], Salvatore Coffa[c], Dave J. Eaglesham[b].

[a] INFM and Dipartimento di Fisica, Università di Catania, C.so Italia, 57, I-95130 Catania, Italy.
[b] Bell Labs, Lucent Technologies, 700 Mountain Avenue, Murray Hill, NJ 07974.
[c] CNR-IMETEM, Stradale Primosole, 50, I-95122, Catania, Italy

Abstract

Several recent experiments assessing the role of impurities (C, O), dopants (P, B) and clustering on defect evolution in ion implanted Si are reviewed. Deep level transient spectroscopy measurements were used to analyze the defect structure in a wide range of ion implantation fluences ($1x10^8$–$5x10^{13}$ cm^{-2}) and annealing temperatures (100-800 °C). By using substrates with a different impurity content and comparing ion implanted and electron irradiated Si samples, many interesting features of defect evolution in Si have been elucidated. It is found that only a small percentage, 4-16 % depending on ion mass, of the Frenkel pairs generated by the beam escape direct recombination and is stored into an equal number of room temperature stable vacancy- (V-) and interstitial-type (I-) defect complexes. Identical defect structures and annealing behavior have been measured in ion implanted (1.2 MeV Si, $1x10^8$–$1x10^{10}/cm^2$) and electron irradiated (9.2 MeV to fluences between 1 and $3x10^{15}/cm^2$) samples in spite of the fact that denser collision cascades are produced by the ions. The O and C content of the substrate plays a major role in determining the point defect migration, the room temperature stable defect structures and their annealing behavior. Annealing at temperatures up to 300 °C produces a concomitant reduction of the I- and V-type defect complexes concentration, demonstrating that defect annihilation occurs preferentially in the bulk. At temperatures above 300 °C, when all V-type complexes have been annealed out, ion implanted samples present a residual I-type damage, storing 2-3 I per implanted ion. This unbalance is not observed in electron irradiated samples and it is a direct consequence of the extra implanted ion. The simple point defect structures produced at low ion fluence ($1x10^8$-$1x10^{11}$ $/cm^2$) anneal at ~ 550 °C. At higher fluences (~ 10^{12}-10^{13} $/cm^2$) and for annealing temperatures above 500 °C the deep level spectrum is dominated by two signatures at E_V+0.33 eV and at E_V+0.52 eV that we have associated to Si interstitial clusters. Impurities (C, O and B) play a role in determining nucleation kinetics of these defects, but they are not their main constituents. The dissolution temperature of these clusters indicates that they might store the interstitials that drive transient enhanced diffusion phenomena occurring in the absence of extended defects. Finally, at higher implantation fluence, a signature of extended defects is observed and associated to the presence of {311} defects detected by transmission electron microscopy analyses.

Introduction

Ion implantation is widely used in the processing of VLSI Si devices. However, ion beam damage is responsible of several phenomena, such as transient enhanced diffusion (TED) [1] and extended defects formation [2], which severely hamper our ability to fabricate sub-micron devices. In order to understand and model these processes, a full comprehension of how ion implantation induced defects form and evolve as a function of the implantation dose and thermal processing is required.

In spite of the widespread use of ion implantation in Si, most of our current knowledge of defect structure and annealing behaviour still relies on the detailed investigations performed [3, 4, 5, 6] during the past 20 years on electron-irradiated silicon. In these studies, the structure and annealing behavior of point defects such as divacancy (VV), oxygen vacancy, (O_iV) and carbon-oxygen (C_iO_i), were assessed, using photoluminescence, deep level transient spectroscopy (DLTS), and electron paramagnetic

Mat. Res. Soc. Symp. Proc. Vol. 504 © 1998 Materials Research Society

resonance analyses. In the last few years, the purity of the Si substrate has increased considerably, and it is now possible to grow wafers with an oxygen and carbon content comparable or lower than the dopant concentration. Since impurities are effective traps for Frenkel pairs generated by the beam, it is reasonable to expect a different evolution of defects in these pure materials [7]. Moreover, although recent DLTS studies [8,9] show that the same defect structures are produced in Si by both ions and electrons, several issues certainly need to be explored in more detail. A significant difference is, in fact, expected between the damage evolution in ion implanted and in electron irradiated Si. It is known that the defect profile for ion implanted samples is not spatially uniform, as in the electron irradiated case, but the damage is mainly localised in a well defined peak at the end of range. Also the density of collisional events is orders of magnitude higher for ions than for electrons. As a result, room temperature annihilation and defect clustering [10] can be greatly favored in ion implanted samples.

Furthermore, while electron irradiation produces equal numbers of vacancies and self-interstitials, ion implantation produces an imbalance between vacancies and interstitials caused by the presence of the extra-incorporated ion. This last observation has noticeable consequences and provides the basis for the +1 model, [11, 12] which is used to describe interstitial clustering, and all the related phenomena occurring for high fluence and high temperature annealing. In this model, it is assumed that extensive recombination of vacancies and interstitials occurs until only the extra ion is left.

The interstitial excess caused by the extra ion presence drives the Transient Enhanced Diffusion (TED) of dopants. Indeed, detailed TEM analyses and B diffusion experiments have demonstrated that release of the interstitials stored into {311} extended defects, drive B enhanced diffusion. The number of interstitials stored in these defects equals the total number of implanted ions, providing a confirmation of the "plus one" model [13].

However, TED occurs even without the formation and dissolution of extended defects [14], as in the case for low dose implants, or in early stages of the annealing process, before the formation of extended defects. To explain these phenomena, small Si interstitial clusters, not detectable by TEM, have been proposed as the interstitial source for TED. The experimental identification of these clusters could give new inputs to the modeling [15] of transient enhanced diffusion phenomena. The new generation of simulation tools for the design of sub-micron devices, in fact, requires an accurate scientific description of defect-defect and defect-impurity interaction, from simple to extended defects during the various implantation and annealing processes.

Deep Level Transient Spectroscopy (DLTS) has been traditionally used in the low implantation fluence regime and considered unable to provide information in the fluence regime where extensive defect clustering and extended defects formation is observed. In this paper we show that DLTS can be effectively used to monitor defect evolution from simple point defects to extended defects. The aim of this work was to characterize ion implantation damage as a function of the impurity content of the material and in a wide dose and annealing temperature range. Ion implantation induced damage can be divided, based on recent experimental investigations [16], into four groups: *interstitial (I-) and vacancy (V-) type point defect pairs*, obtained in samples implanted to low fluences, $\leq 1x10^9$ Si/cm^2 and stable from room temperature to 300 °C; *interstitial point-like defects*, obtained after annealing at temperatures in the range 300-500 °C for implantation doses of $1x10^9$-$1x10^{11}$ Si/cm^2; *interstitial clusters*, formed after implantation doses $\geq 1x10^{12}$ Si/cm^2 and annealing temperatures $\geq$ 550 °C; and *extended defects*, found after implantation at doses $\geq 2x10^{13}$ Si/cm^2, and annealed for temperatures $\geq$ 680 °C. Experimental results for each of the four groups are presented and discussed.

Experimental

We used p-type (doped with $7x10^{15}$ B/cm^3) and n-type (doped with either $5x10^{13}$ P/cm^3 or with $7x10^{14}$ P/cm^3) Si wafers. Both epitaxial (epi, with an O and C content lower than $1x10^{15}$ /cm^3) and

Czochralski (CZ, with [O]= $7x10^{17}/cm^3$ and [C] ≤ $10^{16}/cm^3$) Si samples were analyzed in order to assess the effect of impurities on defect evolution. Samples were implanted with 1-3 MeV He, to fluences in the range $1x10^8$-$8x10^9/cm^2$ or with 145 keV-1.2 MeV Si to fluences in the range $1x10^9$-$5x10^{13}/cm^2$ or irradiated with 9.2 MeV electrons to a fluence of 1 - $3.5x10^{15}/cm^2$. Thermal anneals at temperatures of 100-680 °C for 30 min-15 hr were performed in flowing He. Finally, Schottky barriers were formed on the samples by evaporating either Ti on p-type Si or AuPd on n-type Si after a dip in HF. In some of the DLTS analyses p^+-n junctions, obtained by B implantation and high temperature diffusion, have been used. The samples were characterized by DLTS measurements using Bio-Rad DL4600 or DL8000 Spectrometers.

Interstitial- and vacancy-type point defect pairs

The point defects (I, V) generated by electron irradiation or ion implantation can migrate through the Si lattice until they either recombine according to the relation I + V = ∅ or are stored in room temperature stable defect complexes. Fig. 1 schematically summarizes what is known on the formation of the principal room temperature defect complexes. A vacancy will migrate until it either finds another vacancy, forming a divacancy, VV, or it pairs with impurities to create V-type point defect structures such as oxygen-vacancy, OV, or phosphorus-vacancy, PV [6, 8].

Silicon self-interstitials create, by the Watkins' exchange mechanism [17], interstitial impurities such as boron interstitial, B_i, and carbon interstitial, C_i. The favored branch of the reaction depends on to the ratio between B and C. These interstitial species diffuse at room temperature until they are trapped by impurities and form interstitial-impurity pairs such as carbon-carbon (C_s-C_i), carbon-oxygen (C_iO_i), carbon-phosphorous (C_i-P_s) if C_i is generated [5, 18]. Instead, if B_i is generated in suitable concentration the formation of boron related defect complexes such as boron-oxygen, B_iO_i, boron-carbon, B_iC_s and boron-boron, B_iB_s, [19, 20, 21] will take place. These simple point defect pairs have been widely characterized and all of them anneal at temperatures below 450 °C. The wealth of published information on the identity, introduction rates, annealing behavior, and DLTS signatures of vacancy and interstitial related point defects in electron irradiated Si provides a firm foundation for a

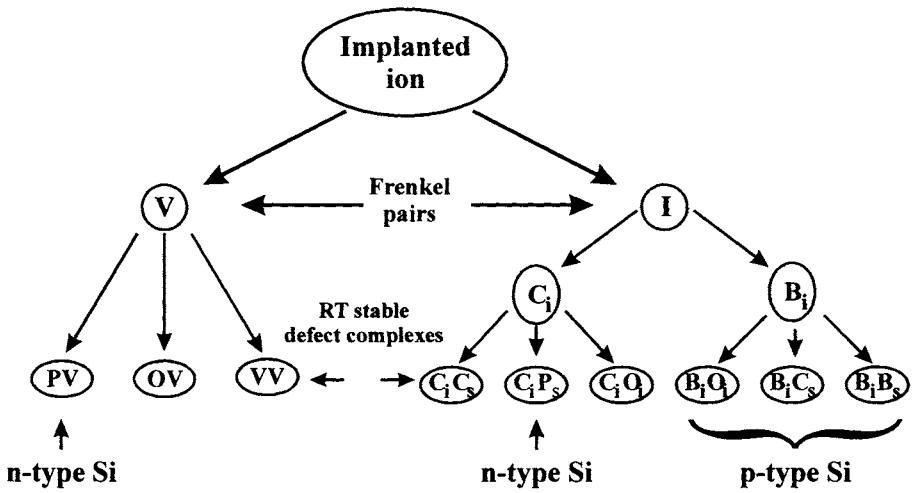

Figure1: *Room temperature stable defect complexes generated by ion implantation with a (light ion) or by electron irradiation in Si.*

comprehensive study of the introduction and evolution of implantation-induced defects in Si.

a. Comparison between electron irradiation and ion implantation in the as-implanted state

In order to apply the knowledge acquired in the last 20 years on electron irradiated samples to ion implantation it is fundamental to compare directly the damage introduced with the two processes. In this study we used Si ions because they do not introduce deep levels in Si and because their collision cascade is diluted. The comparison was performed using the same substrate, thus fixing the impurities (C and O) and dopant concentrations.

The results of the direct comparison between electron irradiation (9.2 MeV, $3.5x10^{15}/cm^2$) and ion implantation (1.2 MeV Si, $1x10^9/cm^2$) are reported in Fig. 2 (*a*) for n-type and (*b*) for p-type samples.

In n-type epitaxial Si, (low C, low O content) the spectra are dominated by V-type defects that introduce deep levels in the upper half of the band gap, such as the oxygen-vacancy, OV E(0.17 eV); the doubly negative charge state of the divacancy, $VV^=$ E(0.22 eV), the singly negative charge state of the divacancy, VV^- E(0.41 eV), and the phosphorous-vacancy, PV E(0.46 eV), normally observed in DLTS after electron irradiation [3]. The spectra of electron irradiated (solid line) and ion implanted (dashed line) Si are almost identical, demonstrating that the same defect structures are introduced. No measurable differences arise as a consequence of the denser ion collision cascade.

The impurity content of the substrate plays a major role in determining the defect structure of as-implanted or as-irradiated Si samples. In silicon with a high concentration of carbon (dot dashed line in Fig. 2*a*), the signal related to P_sC_i, E(0.30 eV), is clearly visible [5].

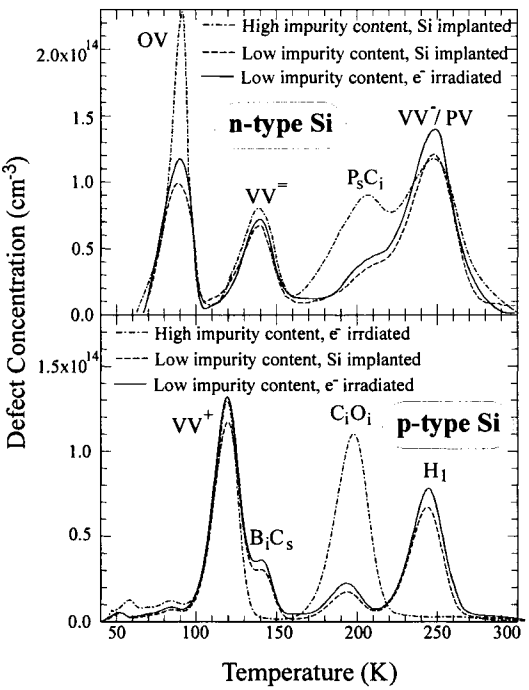

Figure 2: *DLTS spectra of ion implanted or electron irradiated (a) n-type and (b) p-type Si samples with different impurity content.*

In p-type Si, Fig. 2*b*, the DLTS spectrum of a CZ Si sample irradiated with electrons reveals the signatures [4] of the carbon oxygen pair (C_iO_i, at E_V+0.36 eV) and of the positively charged divacancy (VV^+, at E_V+0.21 eV) and, again, the spectrum after irradiation (dot dashed line) and ion implantation (not shown) are the same. Once more, the impurity content plays a major role. In epitaxial Si samples the C_iO_i concentration is much lower than in the CZ sample and two additional defect signatures are present: the boron-carbon pair (B_iC_s, at E_V+0.27 eV) and a B-related defect that contains a single interstitial [7] (H_1, at E_V+0.45 eV). The large differences in the DLTS spectra between epitaxial (solid line) and CZ (dashed dotted line) Si samples spectra can be explained observing that the C_iO_i formation is largely suppressed in epitaxial Si due to the low concentration of both O and C. In this sample B concentration is higher than C concentration and it successfully competes with carbon in storing the self interstitials generated by the irradiation. Self-interstitial will produce, by the Watkins replacement mechanism (see Fig. 1), interstitial B atoms

(B_i) which are then immobilized into defect complexes, as B_iC_s.

These results imply that the dense ion collision cascade and the incorporation of the extra ion do not produce any measurable effect in the as-implanted defect structure. Hence, it is only the impurity content of the material, which is determining the defect structure in the as-implanted state [7].

b. Room temperature migration of interstitials and vacancies

Ion implantation damage is not uniform in all the sample thickness as in the electron irradiation case, but it is well localized at the end of range of the implanted ion. This characteristic of ion implantation can be used to monitor room temperature recombination and migration of vacancies and interstitials [22, 23]. For this study Si substrates with different C and O impurity concentration, were implanted with helium. Helium has a very low atomic mass (4 a.m.u.) and creates a very diluted collision cascade in Si. This minimizes the direct clustering effect within the single ion cascade. Moreover, a very low implantation dose, such as $5x10^8$ He/cm^2, avoids overlapping between different ion track collision cascades. In this study, we used n-type Si and determined the depth profiles of impurity-point defect pairs (OV and P_sC_i) and divacancies.

Depth profiles of the divacancy (●) and oxygen-vacancy (■) defect complexes for a Czochralski Si sample implanted with 1 MeV He, are reported in Fig. 3. The OV concentration in this sample is very high confirming the efficiency of O as a trap for migrating vacancies. Indeed, the OV profile plotted in Fig. 3 has been divided by a factor 1.5 to allow the direct comparison with the VV^- profile. The initial generation of I-V pairs as calculated by Transport of Ion In Matter, TRIM, [24] is also reported as a solid line. The simulated generation curve has been divided by a factor of 22 in order to allow comparison. Important information can be drawn from the figure. A large percentage of interstitials and vacancies generated by the beam anneals during the implant, or immediately after the implantation process. Such extensive recombination occurs within the single cascade, because the implantation dose is well below the threshold to have overlapping between cascades. The concentration of electrically active defects is only ~ 16 % of the total concentration of defects generated by the beam. In spite of the extensive recombination, the depth profile precisely mirrors the Frenkel pair distribution predicted by TRIM. The point defects that escape recombination cannot migrate long distances due to the formation of complexes with other vacancies or pairs with O or P atoms and this effect confirms, once again, that impurities are very efficient traps for point defects.

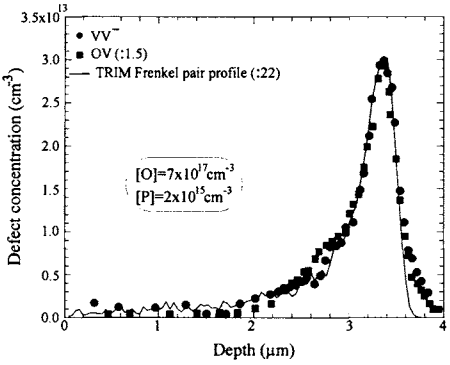

Figure 3: *Depth profiles of VV⁻ (•), and OV (■) for a CZ sample (4 Ωcm, [O]=7x10^{17} /cm^3 and [C]=1x10^{16} /cm^3) implanted with 1 MeV He, 5x10^8 /cm^2. The profiles are compared with a TRIM simulation of the implant profile (solid line).*

The relative importance of defect clustering and impurity trapping can be changed by varying the impurity content in the material and/or changing the mass of the implanted ion [10, 23]. The role played by impurities and dopants on the migration properties of point defects becomes evident when He implants (3 MeV, $5x10^8$cm^{-2}) are performed on substrates having very low impurities and dopant concentrations. In particular, we compared float zoned and epitaxial Si substrates both doped with $5x10^{13}$ P/cm^3. The resulting OV depth concentration profiles are reported in Fig. 4.

The reduction in the sample impurity content, in particular from $7x10^{17}$O/cm^3 of the CZ samples (see Fig. 3) to $2x10^{16}$ O/cm^3 of the FZ or ~ 10^{15} O/cm^3 of the epi samples, results in a significant broadening of

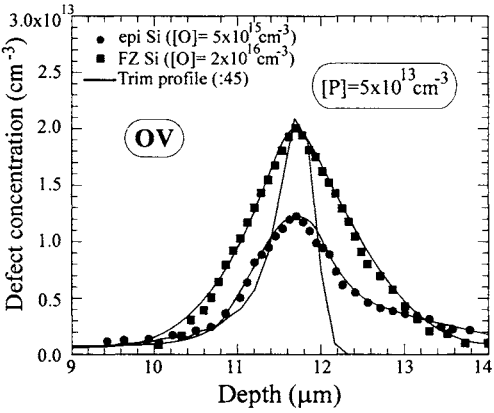

Figure 4: *Depth profiles of OV in samples implanted with 3 MeV He, 5x10^8 /cm^2 on epi Si (of 60 Ωcm, [O] ≤ 5x10^{15} /cm^3 and [C] < 1x10^{16} /cm^3, •); on FZ Si(60 Ωcm, [O] ~ 1x10^{16} /cm^3 and [C] ≤ 1x10^{16} /cm^3, ■). The solid line is a TRIM simulation of the generated Frenkel pairs.*

the OV depth profile (Fig. 4) with respect to the initial defect profile calculated by TRIM (solid line). In a highly pure material, vacancies are free to migrate long distances before they either recombine with interstitials or create stable defect complexes by clustering with other vacancies or pairing with impurities such as O, causing the observed broadening. It should be observed that the experimental depth profiles show a symmetric broadening with respect to the TRIM simulation; moreover, the peak of the defect distribution is deep, ~ 12 μm. Hence, any preferential defect recombination at the surface can be ruled out. A similar depth dependence is found for the VV depth profile, suggesting that for a light ion such as He most of the VV are not formed directly in the collision cascade but result from clustering of two migrating vacancies. [22, 23]. A similar behavior has been observed for interstitial-type defects.

The strong reduction of the sample impurity content also causes a strong reduction in the concentration of vacancy-type defects stable at room temperature. While a value of ~ 16% is observed in CZ Si, the total concentration of V stored in V-type defects is reduced to ~ 3% and ~ 2.6 % for FZ and epi Si, respectively. It occurs because vacancies and interstitials can migrate for a longer distance before being trapped and the probability of annihilation is increased. The experimental results strongly suggest that the room temperature defect migration is in this case a trap limited process where free migrating vacancies are trapped by O and a trapping radius of ~ 1 Å has been measured [23].

c. Annealing behavior of I- and V-type defect complexes

Role of the impurity content

A reduction in impurity content can also change the annealing rate and, hence, the thermal stability of room temperature stable defects. In particular, annealing of defect complexes is the result of either thermal dissociation or annihilation by point defects released by the dissociation of less stable defect structures. The dependence of the annealing temperature on the impurity content is known for some defect complexes, such as the VV [25] and the B_iC_s [20]. We demonstrated [7] that also the C_iO_i complex dissolution temperature is dependent on the impurity content of the sample. The isochronal anneal of the C_iO_i pair for three electron irradiated samples with different impurity concentrations is reported in Fig. 5. The epitaxial (•) and the CZ Si (■) used in this study have a lower carbon concentration, [C] ≤ 10^{16} /cm^3, than the CZ (▲) used in previous electron irradiation studies [20], [C] = 6x10^{16} /cm^3. For this high C sample we also report the annealing behavior of the C_i (★) which was not detected in our other epitaxial and CZ samples. The annealing curve of the C_iO_i complex in this high C CZ sample shows the behavior typically reported for this defect. At 100 °C its concentration increases as the C_i diffuses and pairs with the O, present in high concentration, producing more C_iO_i. The concentration of C_iO_i remains stable up to 250 °C and next decreases slightly in the range 250-350 °C (probably due to annihilation by free vacancies released by the dissolution of divacancies). Finally, complete dissolution of the C_iO_i occurs at 400 °C. The stability of the C_iO_i defect is a consequence of

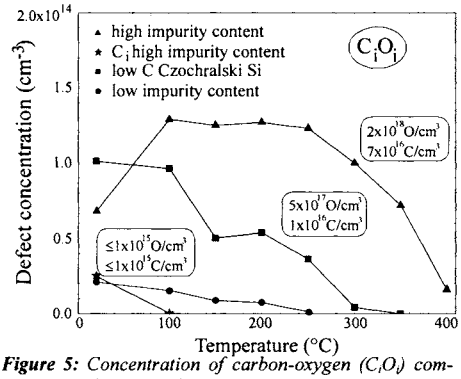

Figure 5: *Concentration of carbon-oxygen (C_iO_i) complexes, as obtained from DLTS, is reported as a function of annealing temperature for epitaxial Si (•) and CZ Si (■). In addition the annealing behavior of C_iO_i (▲) and carbon-interstitial C_i (★) defects in a CZ sample with a higher C content [20] are also reported. All the samples were irradiated with 9.2 MeV electrons to a fluence of 3.5x10^{15}/cm^2.*

both the high binding energy of the two impurity atoms and of the strong back reaction which competes with dissociation. Indeed, in Si with high O concentrations, when a C_iO_i is dissociated the released C_i will have a strong chance to pair again with O.

In epitaxial Si, having a low concentration (≤ 10^{15}/cm^3) of both C and O, the concentration of C_iO_i pairs is greatly reduced since, as shown in Fig. 2*b*, most of the interstitials are expected to be stored into different, B_i related, complexes. B_i-related complexes dissociate at T < 400 °C [7] releasing free B_i. These B interstitials can recombine with vacancy type defects, releasing free vacancies which then produce the dissolution of the C_iO_i defects. In addition, the dissociation of a C_iO_i complex is not balanced by a back-reaction, because the released C_i has little probability of pairing again with O in the epitaxial material. Complete annealing of C_iO_i is achieved at 250 °C. The annealing temperature of the C_iO_i in the low C CZ is intermediate to that of the high C CZ and of the epitaxial Si. Once more C and B compete for the capture of interstitials and the formation of stable defects. The presence of B_i stored in room temperature stable defects will again result in a different annealing behavior of the C_iO_i complex.

Role of the extra implanted ion

The concentration of *V- and I-type point defect pairs* (i.e. VV, C_iO_i,) can be measured by DLTS. Hence, the number of I and V stored in these defects can be counted [26, 27]. We have analyzed the annealing behavior of V-type and I-type point defects in ion implanted and electron irradiated Si samples. We determined the total concentration of vacancies by adding the concentration of the VV (multiplied by a factor two since two vacancies participate to the VV formation) and of the OV. This last contribution is the only one derived from n-type Si spectra since the OV signature is not detectable in p-type samples. The total interstitial concentration is obtained by adding the concentrations of C_iO_i, B_iC_s and H_1. The results are reported in Fig. 6 for both I-type (■) and V-type (▲) defects, calculated for ion implanted samples isochronally (30 min) annealed at temperatures in the range 100-550 °C, in 50 °C steps. The lines, solid for interstitials and dotted and dashed for

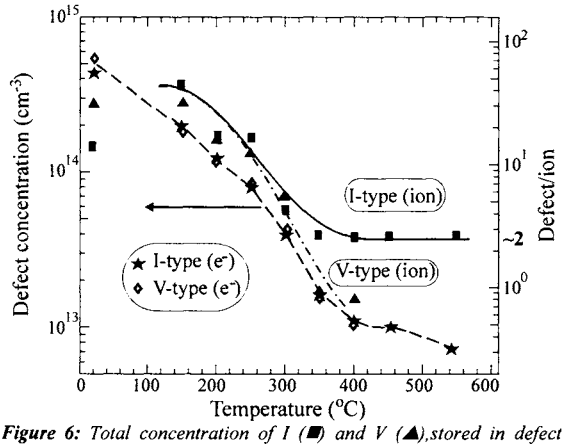

Figure 6: *Total concentration of I (■) and V (▲),stored in defect complexes, as a function of annealing temperature for epi Si implanted with 1.2 MeV Si, 1x10^9/cm^2 and total concentration of I (★) and V (◊) stored in defect complexes for electron irradiated epi Si with 3.5x10^{15}/cm^2, 9.2 MeV.*

vacancies, are only guides to the eye. The right hand scale of the plot represents the number of defects per implanted ion, N, calculated as:

$$N = \frac{C_d x}{\Phi} \qquad (1)$$

where C_d is the average defect concentration in the region probed during the DLTS measurements, x is the thickness of this region (~ 1 μm) and Φ is the implanted fluence ($1x10^9$ /cm^2, in Fig. 6).

Although each ion produces ~ 2500 Frenkel pairs (as calculated by TRIM [24]), only ~ 60 per ion escape recombination and form room temperature stable defects. Thermal annealing at temperatures up to 300 °C produce a concomitant annealing of I and V-type defects. Indeed, an equal number of V-type and I-type defects remain although their absolute concentration has been reduced by approximately one order of magnitude. This confirms that, as expected from Monte Carlo simulations [15], most of the defect recombination occurs in the bulk, thus maintaining the balance between interstitials and vacancies. If surface annihilation of I or V had been dominant, the balance between vacancies and interstitials would not have been maintained.

At temperature above 300 °C all of the vacancy-type clusters have been annealed out, but a measurable number of interstitials (~ 3 per implanted ion) is still present in the samples. We suggest that this unbalance between interstitial and vacancy-type defects is due to the extra incorporated ion [11], and it only becomes experimentally detectable when most of the vacancies have recombined. This hypothesis is confirmed by the observation that this imbalance was not observed in electron irradiated samples where I- (★) and V-type (◊) defects continue to anneal concomitantly. Despite the fact that the two samples have the same as implanted spectrum (see Fig. 2*b*), after annealing at 350 °C the difference in the two samples is experimentally detectable.

Interstitial point-like defects

It is now interesting to apply the defect counting method we developed to samples implanted at higher fluences. Implantation at high fluences results in the deterioration of the junction characteristics and in a defect concentration comparable or higher than the doping concentration. It is not possible to perform DLTS measurements in the as-implanted samples. However, after annealing at 400 °C, most of the damage recovers and DLTS measurements are again possible. Is this region, at annealing temperatures of 350-500 °C after all the vacancies anneal, *interstitial point-like defects* form. These point defects store the interstitial "excess" caused by the presence of the extra ion.

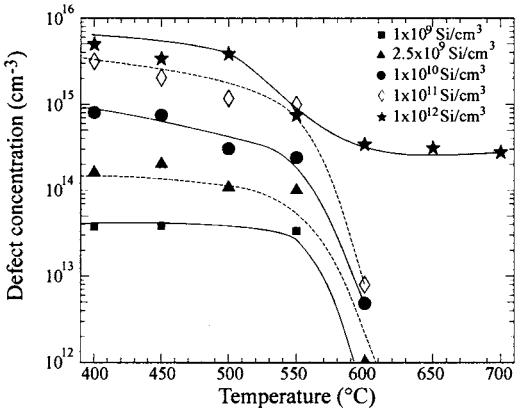

Figure 7: *Residual defects concentration as a function of the temperature for epitaxial Si implanted with 1.2 MeV Si at doses of: 1x10^{9}cm^{-2} (■), 2.5x10^9 cm^{-2} (▲), 1x10^{10} cm^{-2} (●), 1x10^{11} cm^{-2} (◊), 1x10^{12} cm^{-2} (★).*

In Fig. 7 we summarize the results of defect counting on samples that have been annealed for 30 min at temperatures in the range 400-700 °C.

Si samples implanted with 1.2 MeV Si at fluences of 1x10^{9}cm^{-2} (■), 2.5x10^{9}cm^{-2} (▲), 1x10^{10} cm^{-2} (●), 1x10^{11} cm^{-2} (◊), 1x10^{12} cm^{-2} (★). The solid and dashed lines are used as a guide to the eye. For low fluences (up to 1x10^{11} cm^{-2}) the defect concentration increase roughly linearly with ion fluence so that, the number of interstitial per ion, calculated